International Orthopaedics (SICOT) (2013) 37:911–917
DOI 10.1007/s00264-013-1825-5

ORIGINAL ARTICLE

Morphological characteristics of split-depression fractures of the lateral tibial plateau (Schatzker type II): a computer-tomography–based study

Qilin Zhai · Congfeng Luo · Yi Zhu · Ling Yao · Chengfang Hu · Bingfang Zeng · Changqing Zhang

Received: 17 January 2013 / Accepted: 1 February 2013 / Published online: 22 February 2013

Abstract
Purpose The objective of this study was to evaluate the morphological characteristics of lateral tibial plateau split-depression fractures (Schatzker type II).
Methods A retrospective analysis of radiographic and computed tomographic (CT) data of lateral tibial plateau split-depression fractures from January 2009 to December 2010 was conducted in a level 1 trauma centre. The discontinuity arc, angle of depression centre (ADC), anterior-posterior position of articular depression centre (APDC), surface area percentage (SAP), sagittal angulation and depression depth were measured on CT images using the Picture Archiving and Communication System.
Results Based on the integrity of posterolateral wall and discontinuity arc, 140 cases of Schatzker type II fracture were divided into two subtypes: intact group (69 cases) and broken group (71 cases). The fracture of the intact group was located in the anterior part of the lateral plateau, the average ADC was 72.13°, APDC was 43.25 % of sagittal diameter, SAP was 22.16 % of total plateau, sagittal angulation was 6.59°and depression depth was 10.80 mm. Of the broken group, the average ADC, APDC, SAP, sagittal angulation and depression depth was 92.45°, 61.84 %, 22.63 %, 9.00° and 10.78 mm, respectively. Forty-seven cases in the broken group had a posterolateral fragment and 15 cases among them had articular depression centered in the posterolateral region. The difference in ADC, APDC and sagittal angulation between the two groups was statistically significant ($p<0.05$), while no significant difference was observed for SAP and depression depth.
Conclusions Of all the 140 cases in this study, 10.7 % are located in the posterolateral region. An appropriate operative approach and fixation method should be selected based on the individual morphological characteristics of lateral plateau fractures.

Electronic supplementary material The online version of this article (doi:10.1007/s00264-013-1825-5) contains supplementary material, which is available to authorised users.

Q. Zhai · C. Luo (✉) · Y. Zhu · L. Yao · C. Hu · B. Zeng · C. Zhang
Department of Orthopaedic Surgery, Shanghai Sixth People's Hospital, Shanghai Jiaotong University, No.600 Yishan Road, Shanghai, China
e-mail: cong_fengl@yahoo.com.cn

Introduction

Lateral tibial plateau split-depression fracture (Schatzker type II, AO/OTA Type B3) is the most common fracture type encountered clinically, and accounts for 25–33 % of all tibial plateau fractures [1–4]. The fracture morphology of this type is often described in anterior-posterior position, and lateral buttress plating is widely recommended [5–7]. Compared with plain radiographs, computed tomography (CT) scans can provide detailed information on intra-articular fractures. With the widespread use of CT, it has been found that in some cases, the fracture line may appear on the coronal plane and the split-depression fracture may be restricted in the posterolateral region, which is different from ordinary Schatzker type II fractures, as the visualisation of the fracture site was obstructed by the fibular head [8–10]. Inadequate vision or assessment of the fracture may lead

to failure of primary fixation, and furthermore, secondary articular depression, valgus deformity and deterioration in the long-term [11].

Thorough understanding of the fracture morphology can help orthopaedic surgeons understand the accurate mechanism of injury and plan appropriate surgical procedures. However, to our knowledge, there has not been a study that has analysed three-dimensional morphology of lateral tibial plateau split-depression fractures or the incidence of the posterolateral fragment in this type. Therefore, in this study, three-dimensional CT images of the patients who suffered from Schatzker type II fracture were analysed retrospectively to clarify the morphological characteristics of these fractures.

Patients and methods

The retrospective study was conducted at a level 1 trauma centre. A total of 151 adult patients of Schatzker type II fractures between January 2009 and December 2010 were retrieved from our institution's trauma database with the approval of our institution's Human Subject Review Board. Fracture types visualised by X-ray were the consensus of two observers (Q. Z. and Y. Z.) and were verified by senior surgeons postoperatively. Exclusion criteria were fractures in medial plateau, inadequate imaging documentation (incomplete CT images) and previous knee surgery and/or existing knee deformity. Finally, ten patients having fracture in medial and one without CT images were identified, and this left 140 fractures during the study period. Of these cases, 82 were male and 58 were female, with an average age of 49 years (range, 21–80 years). The causes of injury included car accident in 17 cases, electric bicycle traffic accidents in 83 cases, fall from a height in three cases, and simple fall injury in 37 cases. Fourteen cases had concomitant ipsilateral proximal fibular fractures.

The images were evaluated on clinical Picture Archiving and Communication System (PACS) workstations by two orthopaedic trauma surgeons and one radiologist specialising in musculoskeletal radiology. All measurements were reviewed simultaneously by the three observers and agreement was reached by consensus.

Morphological assessment: CT axial images

Reference line

Two projection points in the CT transverse view were found: Point O is the projection of the midpoint of two tibial intercondylar eminences and Point A is the projection of the most anterior point of the tibial tuberosity. We connected these two points and extended to the posterior edge (Point B). The segment AB was divided into 100 small segments of same length and used as a ruler (Fig. 1, bold line).

Discontinuity arc

Beginning at Point A, along the rim of lateral tibial plateau clockwise, the curve between the start and termination point of broken cortex was connected, which was defined as the discontinuity arc (Fig. 1, bold curve). The angle between line OA and the line that was formed by connecting the first broken cortex point was measured; so was the termination point (Fig. 1, white dotted lines). The position of the termination point was compared with proximal tibia-fibular joint, anterior or posterior, and was recorded.

Location of articular depression centre

The centre (Point C) of articular depression region, an irregular closed polygon, was calculated by a computer program developed by ourselves that was based on calculus, and its horizontal and vertical ordinates were Cx and Cy.

$$C_x = \frac{1}{6A}\sum_{i=0}^{N-1}(x_i + x_{i-1})(x_i y_{i+1} - x_{i+1} y_i)$$

$$C_y = \frac{1}{6A}\sum_{i=0}^{N-1}(y_i + y_{i+1})(x_i y_{i+1} - x_{i+1} y_i)$$

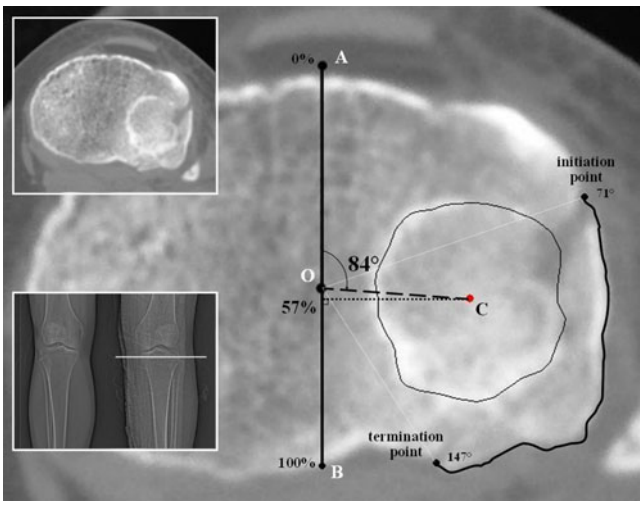

Fig. 1 Radiographic measurements: in computed tomography (CT) transverse view. Two smaller figures showed the section and fracture. Point O and Point A: projections of the midpoint of two tibial intercondylar eminences and the most anterior point of tibial tuberosity. Point B: intersection of line AO and posterior edge. Point C: centre of articular depression region. In this case, the discontinuity arc is from 71° to 147°, the angle of depression centre (ADC) was 84°, the anterior-posterior position of depression centre (APDC) was 57 %, and the posterolateral cortex is broken

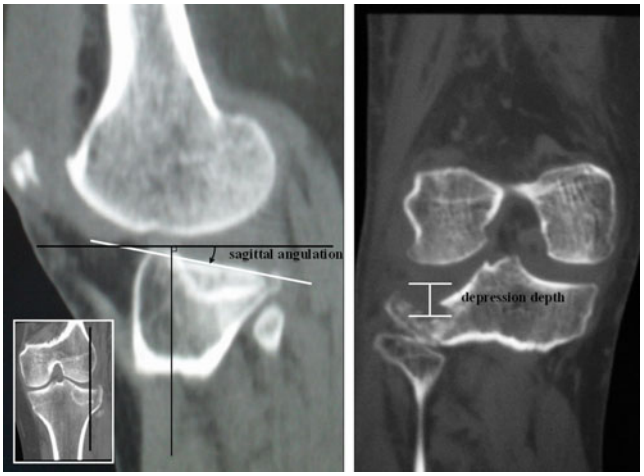

Fig. 2 Radiographic measurements: in computed tomography (CT) sagittal and coronal view. In this case, the sagittal angulation was 11°, the depression depth was 10 mm

$$A = \frac{1}{2}\sum_{i=0}^{N-1}(x_i y_{i+1} - x_{i+1} y_i)$$

Point C was located automatically by computer, while the outline of depression region was inputted. The angle of depression centre (ADC) was determined by measuring the angle between segment OA and OC (Fig. 1, 84°), and the anterior-posterior position of the depression centre (APDC) was measured by the calibrations on the 'ruler' AB (Fig. 1, 57 %).

Area of articular depression

The area of articular depression region and entire tibial plateau were measured on the same section on which the fibular head first appeared. The surface area percentage (SAP) was the percentage of articular depression region of the entire plateau.

Morphological assessment: CT sagittal and coronal Images

Sagittal angulation

Using the method proposed by Streubel et al. [12], a line perpendicular to the tibial axis was drawn, and the lateral plateau sagittal angulation was the angle between it and a line parallel to the articular surface (Fig. 2, left).

Depression depth

Using the coronal CT reformation, the depression depth was obtained by measuring the distance from the normal articular surface to the most depressed articular surface (Fig. 2).

Statistical methods

All statistical analyses were performed using SPSS 17.0 software (SPSS Inc., Chicago, IL, USA). The descriptive statistics and scatter plots were employed for morphological data, and the parameters between the two groups were compared using the two independent sample *t* test. Fisher's exact test was used to compare the ratio of concomitant fibular fracture. Differences were considered significant if the P value was less than 0.05.

Results

The mean ADC, APDC, SAP, sagittal angulation and depression depth are shown in Table 1. According to the position of the discontinuity arc's terminal point, the 140 cases of lateral tibial plateau split-depression fractures in criteria were classified into two broad categories: (1) 69 cases were completely anterior to the tibio-fibular joint, meaning an intact posterolateral cortex (Fig. 3); (2) 71 cases were partially or completely posterior to the tibio-fibular joint, implying a broken posterolateral wall (Fig. 4).

Of the 69 cases with an intact posterolateral wall, the mean ADC was 72.13±9.81°, APDC was 43.25±6.27 %, SAP was 22.16±5.83 %, sagittal angulation was 6.59±1.56° and depression depth was 10.80±3.16 mm. One case in these 69 had a concomitant proximal fibular fracture.

Of the 71 cases with a broken posterolateral wall, the average ADC, APDC, SAP, sagittal angulation and depression depth was 92.45±17.67°, 61.84±12.44 %, 22.63±7.85 %, 9.00±2.68° and 10.78±2.05 mm, respectively.

Table 1 The results of radiographic measurements

Posterolateral wall	*n*	ADC	APDC	SAP	Sagittal angulation	Depression depth	Fibular fracture
Intact	69	72.13±9.81	43.25±6.27	22.16±5.83	6.59±1.56	10.80±3.16	1
Broken	71	92.45±17.67	61.84±12.44	22.63±7.85	9.00±2.68	10.78±2.05	13
Total	140	83.25±17.75	53.34±13.69	22.40±6.91	7.89±2.17	11.33±2.28	14

ADC angle of depression centre; APDC anterior-posterior position of depression centre; SAP surface area percentage

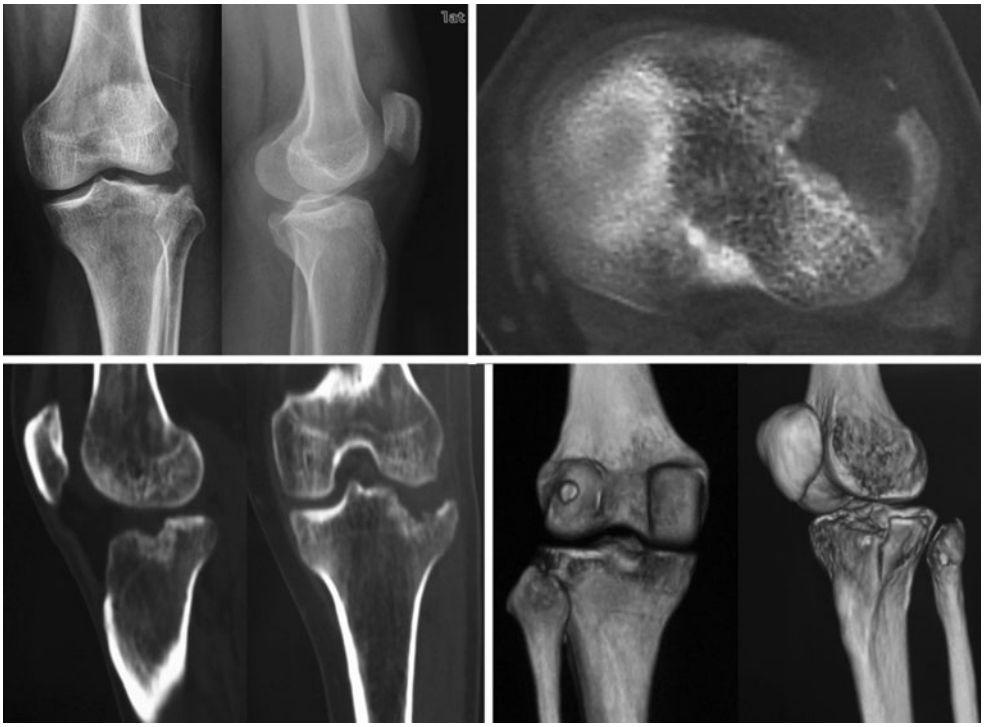

Fig. 3 X ray and three dimensional computed tomography (CT) view of one case in intact posterolateral group. The split fracture and articular depression are in the anterolateral region and indicate a traditional approach

Thirteen cases of the 71 had concomitant proximal fibular fracture. Further analysis of this group, 24 cases demonstrated merely a fracture line on the posterolateral wall; the other 47 cases had one or more posterolateral fragment(s). Fifteen cases had a posterolateral fragment, as well as the articular depression centered in the posterolateral region (Fig. 5).

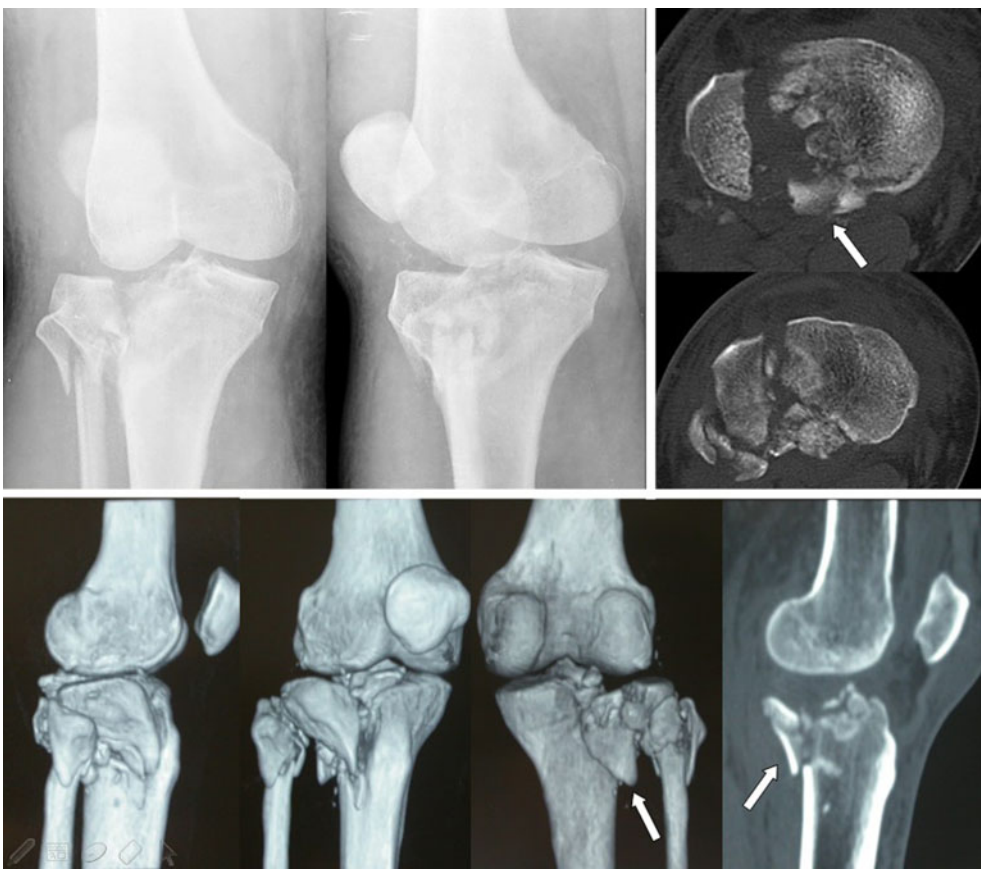

Fig. 4 X ray and three dimensional computed tomography (CT) view of one case in broken posterolateral cortex group. The centre of articular depression is in the posterolateral region and a displaced posterolateral fragment can be seen (white arrow), which is difficult to reduce and fix by a traditional anterolateral approach

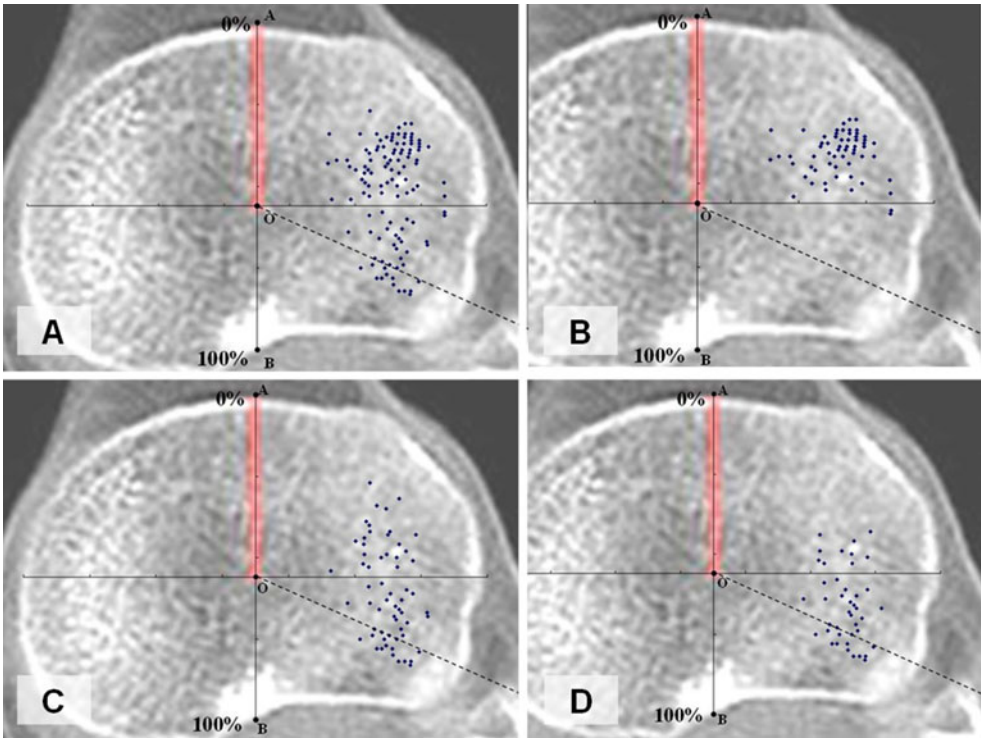

Fig. 5 The scatterplots of articular depression centre. A: 140 cases. B: 69 cases of intact posterolateral wall. C: 71 cases of broken posterolateral cortex. D:47 cases have posterolateral fragment, and 15 centres in the posterolateral region

Between the groups of intact and broken posterolateral wall, the rate of concomitant proximal fibular fracture and the parameters of ADC, APDC and sagittal angulation had a significant difference; however, the SAP and depression depth showed no significant difference (Table 2).

Discussion

Schatzker classification is one of the widest accepted classifications of tibial plateau fracture, and its type II has two basic manifestations in lateral tibial plateau: split fracture and articular depression. Because of the anatomical characteristics of the lateral plateau, convex to the femur and a substantial proportion of cancellous bone, there is usually more than one fracture fragment [13]. Therefore, it is difficult to analyse the direction of fracture line using the methods of previous authors for the medial counterpart [14–16]. In this study, we focused on the osseous rim of the lateral plateau and applied the concept of a discontinuity arc to describe the split fracture. This method made sense, because it indicated the fracture in the lateral plateau wall and corresponded to the concept of buttress fixation popular in clinical practice. Unlike the split fracture, the morphological characteristics of articular depression are relatively easy to analyse: the location, area and depth of it can be sufficiently described by ADC, APDC, SAP and depression depth in this study.

For most of Schatzker type II fractures, the anterior or anterolateral approach is standard and efficient. This study also proved that about half (69/140) of the lateral split-depression fractures are totally in the anterolateral region, unlikely be affected by the fibular head (Fig. 3). However, when the fracture line extends to the posterior aspect of proximal tibiofibular joint in some cases, the visualisation of the fracture may be obstructed by the fibular head. Several previous studies have already discovered this kind of fracture and labelled the low-energy posterolateral fracture of the tibial plateau as an uncommon injury [8, 10, 17, 18]. Yet, there was no analysis of precise incidence or the fracture morphological characteristics. In this study, we found that among the 140 cases in criteria, 47 cases

Table 2 Comparison of the results between two groups

Posterolateral wall	*n*		ADC	APDC	SAP	Sagittal angulation	Depression depth	Fibular fracture
Intact	69							
		P	< 0.0001	< 0.0001	0.6888	< 0.0001	0.9645	0.0011
Broken	71							

ADC angle of depression centre; APDC anterior-posterior position of depression centre; SAP surface area percentage

(33.6 %) had a posterolateral fragment, and 15 cases (10.7 %) had both posterolateral fragment and posterolateral-centered articular depression (Figs. 4, 5). Apart from the surgical vision, a recent biomechanical test has shown that the posterior buttress plate is more stable than the lateral type in fixation of a posterolateral shearing fragment [20]. Therefore, the preoperation plan for these fifteen cases may be different from the usual lateral split-depression fractures, lateral or prone position, and surgical instruments for fenestration or fibular head osteotomy might be considered [11, 19, 21, 22].

According to the integrity of posterolateral wall, the cases were divided into intact and broken group in this study. Between the two groups, the area and depth of articular depression, which related to the trauma energy [1, 3], are not significantly different. Meanwhile, the location of articular depression, the rate of concomitant fibular fracture and sagittal angulation between the two groups are significantly different. It was pointed out by Tanifuji et al. that the centre of femoral condyle moves backwards when the knee is in flexion [23]. We suspected that the location of articular depression and occurrence of a posterolateral fragment would be closely related to the angle of knee flexion and the knee joint movement trend at the moment of injury. Although this can be confirmed by collecting trauma history, it requires further biomechanical experiments for validation.

CT scanning is recommended to assess morphological characteristics for tibial plateau fractures, especially for comminuted cases [24]. Previous studies have compared the reliability and reproducibility of different classifications under CT scanning and X-ray, and demonstrated the advantages of CT scanning [24, 25]. In this study, ten cases that were classified as Schatzker type II fractures by X-ray have revealed a fracture line in medial plateau under CT scanning and verified in operation, so these fractures should be classified into Schatzker type V. Sufficient attention should be given to these ten excluded cases with a fracture pattern that was not appreciated on plain films (Fig. 6). Even though correctly classified into the same type, 15 lateral split-depression fractures with both posterolateral fragment and posterolateral-centered articular depression showed some morphological differences from ordinary type II fractures. Although agreement on fracture classification is important, we maintain that an appropriate treatment plan based on a thorough understanding of the fracture morphology with the use of three-dimensional CT images is more important.

Our study has two potential limitations. First, the research institution is the leading trauma centre in southern China for high-severity fractures; therefore, the proportion of severe and difficult-to-treat patients may be higher than it should be, and the ratio of the posterolateral fractures probably did not represent the true ratio in the general population. Second, we only focused on the bone structure and neglected the soft tissue

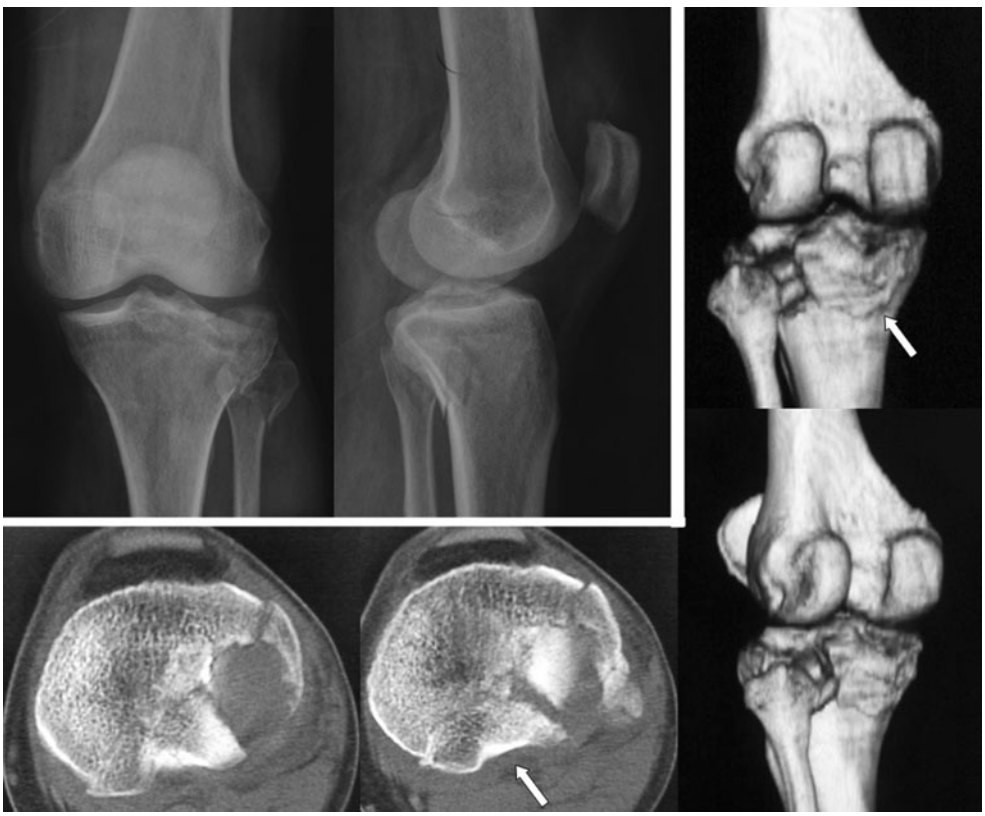

Fig. 6 One case was classified as Schatzker type II fracture by X ray examination, but a fracture line in medial plateau (white arrow) was found under computed tomography (CT) scanning, and verified at operation

injury, which also plays an important role in the posterolateral aspect of the tibial plateau. In addition, because haematoma may lead to a high false positive rate of MRI, in almost every hospital, CT scan can be taken at any time, but there is usually a long waiting time for MRI.

References

1. Kennedy JC, Bailey WH (1968) Experimental tibial-plateau fractures. Studies of the mechanism and a classification. J Bone Joint Surg Am. 50(8):1522–1534
2. Marsh JL, Slongo TF, Agel J, Broderick JS, Creevey W, DeCoster TA, Prokuski L, Sirkin MS, Ziran B, Henley B, Audigé L (2007) Fracture and Dislocation Classification Compendium - 2007: Orthopaedic Trauma Association Classification, Database and Outcomes Committee. J Orthop Trauma 21(10 Su ppl):S1–S133
3. Schatzker J, McBroom R, Bruce D (1979) The tibial plateau fracture. The Toronto experience 1968-1975. Clin Orthop Relat Res 138:94–104
4. Zhu Y, Yang G, Luo CF, Smith WR, Hu CF, Gao H, Zhong B, Zeng BF (2012) Computed tomography-based Three-Column Classification in tibial plateau fractures: introduction of its utility and assessment of its reproducibility. J Trauma Acute Care Surg 73 (3):731–737. doi:10.1097/TA.0b013e31825c17e7
5. Karunakar MA, Egol KA, Peindl R, Harrow ME, Bosse MJ, Kellam JF (2002) Split depression tibial plateau fractures: a biomechanical study. J Orthop Trauma 16(3):172–177
6. Egol KA (2005) Split Depression Posterolateral Tibial Plateau Fracture: Direct Open Reduction and Internal Fixation. Techniques in Knee Surgery 4(4):257–263
7. Egol KA, Tejwani NC, Capla EL, Wolinsky PL, Koval KJ (2005) Staged management of high-energy proximal tibia fractures (OTA types 41): the results of a prospective, standardized protocol. J Orthop Trauma 19(7):448–455
8. Tao J, Hang DH, Wang QG, Gao W, Zhu LB, Wu XF, Gao KD (2008) The posterolateral shearing tibial plateau fracture: treatment and results via a modified posterolateral approach. Knee 15 (6):473–479. doi:10.1016/j.knee.2008.07.004
9. Solomon LB, Stevenson AW, Baird RP, Pohl AP (2010) Posterolateral transfibular approach to tibial plateau fractures: technique, results, and rationale. J Orthop Trauma 24(8):505–514. doi:10.1097/BOT.0b013e3181ccba4b
10. Chang SM, Zheng HP, Li HF, Jia YW, Huang YG, Wang X, Yu GR (2009) Treatment of isolated posterior coronal fracture of the lateral tibial plateau through posterolateral approach for direct exposure and buttress plate fixation. Arch Orthop Trauma Surg 129(7):955–962. doi:10.1007/s00402-009-0829-5
11. Frosch KH, Balcarek P, Walde T, Stürmer KM (2010) A new posterolateral approach without fibula osteotomy for the treatment of tibial plateau fractures. J Orthop Trauma 24(8):515–520. doi:10.1097/BOT.0b013e3181e5e17d
12. Streubel PN, Glasgow D, Wong A, Barei DP, Ricci WM, Gardner MJ (2011) Sagittal Plane Deformity in Bicondylar Tibial Plateau Fractures. J Orthop Trauma 25(9):560–565. doi:10.1097/BOT.0b013e318200971d
13. Eggli S, Hartel MJ, Kohl S, Haupt U, Exadaktylos AK, Röder C (2008) Unstable bicondylar tibial plateau fractures a clinical investigation. J Orthop Trauma 22(10):673–679. doi:10.1097/BOT.0b013e31818b1452
14. Higgins TF, Kemper D, Klatt J (2009) Incidence and morphology of the posteromedial fragment in bicondylar tibial plateau fractures. J Orthop Trauma 23(1):45–51. doi:10.1097/BOT.0b013e31818f8dc1
15. Barei DP, O'Mara TJ, Taitsman LA, Dunbar RP, Nork SE (2008) Frequency and fracture morphology of the posteromedial fragment in bicondylar tibial plateau fracture patterns. J Orthop Trauma 22 (3):176–182. doi:10.1097/BOT.0b013e318169ef08
16. Yang G, Zhu Y, Luo C, Putnis S (2012) Morphological characteristics of Schatzker type IV tibial plateau fractures: a computer tomography based study. Int Orthop 36(11):2355–2360. doi:10.1007/s00264-012-1646-y
17. Weil YA, Gardner MJ, Boraiah S, Helfet DL, Lorich DG (2008) Posteromedial supine approach for reduction and fixation of medial and bicondylar tibial plateau fractures. J Orthop Trauma 22 (5):357–362. doi:10.1097/BOT.0b013e318168c72e
18. Carlson DA (2005) Posterior bicondylar tibial plateau fractures. J Orthop Trauma 19(2):73–78
19. Carlson DA (1998) Bicondylar fracture of the posterior aspect of the tibial plateau. A case report and a modified operative approach. J Bone Joint Surg Am 80(7):1049–1052
20. Zhang W, Luo CF, Putnis S, Sun H, Zeng ZM, Zeng BF (2012) Biomechanical analysis of four different fixations for the posterolateral shearing tibial. Knee 19(2):94–98. doi:10.1016/j.knee.2011.02.004
21. Lowe JA, Tejwani N, Yoo BJ, Wolinsky PR (2012) Surgical techniques for complex proximal tibial fractures. Instr Course Lect 61:39–51
22. Luo CF, Sun H, Zhang B, Zeng BF (2010) Three-column fixation for complex tibial plateau fractures. J Orthop Trauma 24(11):683–692. doi:10.1097/BOT.0b013e3181d436f3
23. Tanifuji O, Sato T, Kobayashi K, Mochizuki T, Koga Y, Yamagiwa H, Omori G, Endo N (2011) Three-dimensional in vivo motion analysis of normal knees using single-plane fluoroscopy. J Orthop Sci 16(6):710–718. doi:10.1007/s00776-011-0149-9
24. Chan PS, Klimkiewicz JJ, Luchetti WT, Esterhai JL, Kneeland JB, Dalinka MK, Heppenstall RB (1997) Impact of CT scan on treatment plan and fracture classification of tibial plateau fractures. J Orthop Trauma 11(7):484–489
25. Brunner A, Horisberger M, Ulmar B, Hoffmann A, Babst R (2010) Classification systems for tibial plateau fractures; does computed tomography scanning improve their reliability? Injury 41(2):173–178. doi:10.1016/j.injury.2009.08.016